Light-Scattering Study of Semiflexible Polymer Solutions. 4. *n*-Hexane Solutions of Poly(*n*-hexyl isocyanate)

Yuji Jinbo,[†] Osamu Teranuma,[‡] Masaaki Kanao,[§] and Takahiro Sato*,[⊥]

Department of Macromolecular Science, Osaka University, 1-1 Machinaneyama-cho, Toyonaka, Osaka 560-0043, Japan

Akio Teramoto[⊥]

Department of Applied Chemistry, Faculty of Science and Engineering, Ritsumeikan University, Nojihigashi 1-1-1, Kusatsu, Shiga 525-8577, Japan

Received May 6, 2002

ABSTRACT: Static light-scattering behavior was investigated for semidilute *n*-hexane solutions of poly(*n*-hexyl isocyanate) (PHIC). At 25 °C, the monomer-unit structure factor $\hat{S}(k)$ of the solutions was favorably compared with the generalized Ornstein−Zernike integral equation theory, and the strength of the attractive interaction between PHIC chains in *n*-hexane was estimated to be very weak. On the other hand, after the solutions were quenched at 15 °C, theoretically unexpected enhanced low-angle scattering was observed. While $\hat{S}(k)$ gradually increased with the quenching time, the anomaly disappeared by heating or diluting the solutions. The normal $\hat{S}(k)$ was also recovered by subtracting the anomalous component from $\hat{S}(k)$ of quenched solutions using dynamic light-scattering results. The anomaly in $\hat{S}(k)$ indicates the formation of aggregates or clusters of PHIC chains in quenched solutions. A strong interchain attractive interaction expected in aggregates is in a contrast with the weak interaction among molecularly dispersed PHIC chains.

Introduction

Light scattering is a useful technique to investigate the size, intermolecular interaction, and distribution of polymer chains or their monomer units in solution. For solutions of molecularly dispersed linear polymers, light-scattering theories have been developed to formulate their structure factors $\hat{S}(k)$ with respect to monomer units (k, the magnitude of the scattering vector), which can be used for the analysis of light scattering data to extract important molecular information. For flexible polymers, renormalization group theories were applied to formulate $\hat{S}(k)$ of semidilute solutions.[1−3] On the other hand, $\hat{S}(k)$ of stiff polymer solutions of finite concentrations was formulated by the generalized Ornstein−Zernike integral equation theory (the GOZ theory)[4−7] combined with the scaled particle theory for the wormlike spherocylinder model.[8,9] In this series of papers,[8−10] we demonstrated that the latter theory can successfully describe light-scattering behavior of a typical stiff polymer, poly(*n*-hexyl isocyanate) (PHIC) dissolved in dichloromethane (DCM).

However, we sometimes encounter difficulty in analyzing light-scattering results. Several authors[11−15] reported anomalous low-angle scattering from semidilute solutions of polystyrene, which cannot be explained by the theories available at present. This anomaly makes it difficult to estimate the osmotic compressibility or correlation length from the light-scattering data.

Similar anomaly of static light scattering was observed in semidilute *n*-hexane solutions of PHIC above a critical concentration after quenching to a low temperature, and could not be explained by the GOZ theory. It is known that the *n*-hexane solution of PHIC is a unique system, which forms a thermoreversible gel at a low temperature.[16,17] This behavior forms a striking contrast to the DCM solution of PHIC being transformed into a nematic phase at high concentrations.[18,19] This implies that the intermolecular interaction of PHIC may be quite different in *n*-hexane and DCM.

In this paper, we report the static light-scattering behavior of semidilute *n*-hexane solutions of PHIC measured before and after quenching. Before quenching, $\hat{S}(k)$ values for the *n*-hexane solutions were favorably compared with the GOZ theory as for DCM solutions, and the strength of the attractive interaction between PHIC chains in *n*-hexane was estimated to be very weak. However, theoretically unexpected enhanced low-angle scattering was observed after quenching, which made the analysis of $\hat{S}(k)$ difficult. We have investigated the temperature and polymer concentration dependencies of the anomalous scattering as well as the anomalous solutions by dynamic light scattering combined with static one, and found to recover the nomal scattering, which agrees with the GOZ theory, by heating and diluting the quenched solutions, and also by eliminating the anomalous component from the total $\hat{S}(k)$ using the dynamic light-scattering result. The anomaly may arise from aggregates or clusters of PHIC chains formed in quenched solutions, though the attractive force among PHIC chains is very weak in *n*-hexane before quenching. We briefly discuss the attractive interaction of the PHIC chain on the basis of the theory of the dispersion force.

Experimental Section

Seven fractionated PHIC samples were chosen from our stock. The samples were mixed with *n*-hexane and stirred with

[†] Present address: Graduate School of Engineering, Yamagata University, Yonezawa, Yamagata 992-8510, Japan.
[‡] Present address: Sharp Corporation, 2613-1 Ichinomoto-cho, Tenri, Nara 632, Japan
[§] Present address: Mitsubishi Polyester Film Corporation, 347 Inokuchi, Santo-cho Sakata-gun, Shiga 521-0234, Japan.
[⊥] Also at CREST, Japan Science and Technology.

10.1021/ma020704o CCC: $25.00
Published on Web 12/14/2002

a magnetic bar at ca. 40 °C for 3−4 days. After preparation, the test solutions were kept above 25 °C or quenched at 15 °C for different times and then used for light-scattering measurements. Static light-scattering measurements were made for the test solutions at 25 °C using a Fica 50 light-scattering photometer with vertically polarized 436 and 546 nm light mostly with no analyzer, in the same procedure as in the previous study.[10] For quenched solutions, it was checked that scattering intensities did not change with rising temperature from 15 to 25 °C. The structure factor $\hat{S}(k)$ (for the isotropic scattering) was calculated from the excess Rayleigh ratio R_θ by $\hat{S}(k) = R_\theta/KcM_0$, where K is the optical constant, c is the polymer mass concentration, and M_0 is the molecular weight of the monomer unit (=127). (Here, $\hat{S}(k)$ is the Fourier transform of the total correlation function of *the monomer unit* composing the polymer chain, not that of polymer chain itself.)

The specific refractive index increment $\partial n/\partial c$ included in the optical constant K was measured for PHIC (Sample JP-3-3) in *n*-hexane at 25 °C at c up to 0.10 g/cm^3 by a modified Schultz−Cantow differential refractometer. The results were 0.132 cm^3/g at 436 nm and 0.126 cm^3/g at 546 nm, irrespective of c, which are in good agreements with the results of Murakami et al.[20] obtained in a dilute region.

The temperature-quench experiment was made by transferring cylindrical light-scattering cells with an inner diameter of 22 mm from 25 °C (or higher temperature) to 15 °C baths. The final temperature was atteined within few minutes. Quenched solutions looked transparent and kept fluidity, so that their light-scattering measurements themselves were made without difficulty.

The intensity autocorrelation function $g^{(2)}(t)$ of a *n*-hexane solution of a PHIC sample (JP-3-3) quenched at 15 °C was measured using an ALV/DLS/SLS-5000 light-scattering system equipped by an ALV-5000 multiple tau digital correlator. Vertically polarized light with the wavelength λ_0 of 532 nm emitted from a Nd:YAG laser (model 532, Coherent) was used as the incident light. The relaxation spectrum $A(\tau)$ of $g^{(2)}(t)$ was obtained by the CONTIN analysis, where the range of the relaxation time τ from 1 μs to 10 s were divided into 70 equal intervals in the logarithmic scale.

Results and Discussion

Normal Scattering. Figure 1 shows plots of $\hat{S}(k)^{-1}$ vs k^2 for *n*-hexane solutions of samples JP-3-3 and C-3 of different concentrations at 25 °C. Filled circles indicate $\hat{S}(k)^{-1}$ at infinite dilution, from which the weight-average molecular weight M_w and the radius of gyration $\langle S^2\rangle^{1/2}$ of the samples were estimated.[21] The results of M_w and $\langle S^2\rangle^{1/2}$ for all samples studied are listed in Table 1. The molecular weight dependence of $\langle S^2\rangle^{1/2}$ for our samples agrees with Murakami et al.'s[20] and fits to the theory of Benoit and Doty[22] for the unperturbed wormlike chain with the persistence length $q = 43$ nm and the molar mass per unit contour length $M_L = 730$ nm^{-1}.[23] This unperturbed behavior is due to the stiffness of the PHIC chain, which undergoes no intramolecular excluded-volume effect.

By extrapolating $\hat{S}(k)^{-1}$ in Figure 1 to the zero k, we have estimated $\hat{S}(0)^{-1}$, which is equal to $(M_0/RT)\partial\Pi/\partial c$, where M_0 is the molar mass of the monomeric unit, RT is the gas constant multiplied by the absolute temperature, and Π is the osmotic pressure.[24,25] Figure 2 shows the polymer mass concentration c dependence of $\hat{S}(0)^{-1}$ obtained for *n*-hexane solutions of six PHIC samples (unfilled circles). For samples No-34 and NRX VII-d, $(M_0/RT)\partial\Pi/\partial c$ values were determined by sedimentation equilibrium in a previous study.[26] The results are shown by filled circles in Figure 2. As expected, both filled and unfilled circles for the two samples obey single lines. Table 1 lists the results of the second virial coefficient A_2, estimated from initial slopes of the plots of $\hat{S}(0)^{-1}$ vs c in Figure 2. The values of A_2 are around 9.5 × 10^{-4} cm^3 mol/g^2, independent of M_w, which indicate that *n*-hexane is a good solvent for PHIC. The molecular weight independence of A_2 is characteristic of stiff polymer solutions.[10]

Previously, we[26] demonstrated that $\partial\Pi/\partial c$ data for *n*-hexane solutions of relatively low molecular weight PHIC, obtained by sedimentation equilibrium, were

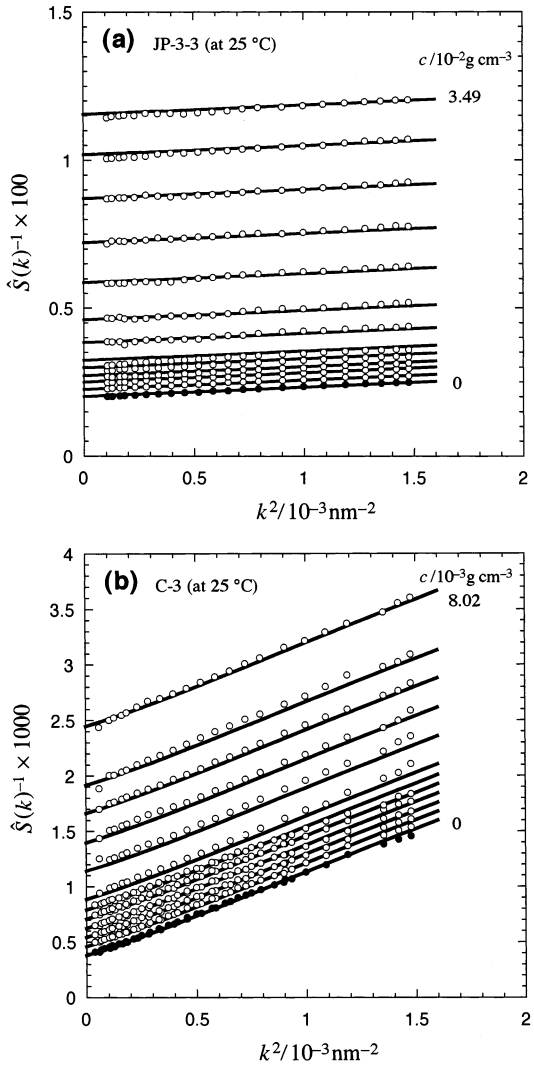

Figure 1. Plots of $\hat{S}(k)^{-1}$ vs k^2 for *n*-hexane solutions of PHIC at 25 °C. (a) Sample JP-3-3, $c/10^{-2}$ g cm^{-3} = 3.49, 3.04, 2.54, 2.01, 1.52, 1.04, 0.738, 0.499, 0.397, 0.287, 0.202, 0.0997, and 0 (from top to bottom). (b) Sample C-3, $c/10^{-3}$ g cm^{-3} = 8.02, 6.00, 5.03, 4.01, 3.01, 2.01, 1.63, 1.30, 0.937, 0.647, 0.323, and 0 (from top to bottom). Solid curves were calculated by the generalized Ornstein−Zernike integral equation theory (cf. eq 1) with $q = 43$ nm, $M_L = 730$ nm^{-1}, $d = 1.10$ nm, and $\delta = -0.08$ nm in panel a and with $q = 41$ nm, $M_L = 750$ nm^{-1}, $d = 1.10$ nm, and $\delta = 0$ nm in panel b.

Table 1. Molecular Characteristics of PHIC Samples Used

sample	$M_w/10^4$	$A_2/10^{-4}$ cm^3 mol g^{-2}	$\langle S^2\rangle^{1/2}$/nm	M_w/M_n[a]
JP-3-3	6.30	9.5	23.0	1.04
No-34	7.94	10.1	26.1	1.03
NRX VII-d	11.7	9.2	35.8	1.07
JP-3−1	18.7	9.7_5	50.6	1.26
C-3	33.4	9.9	70.7	
J-2	48.6	9.4	87.4	
V-1−2	103	8.7	136	

[a] Determined by size-exclusion chromatography.

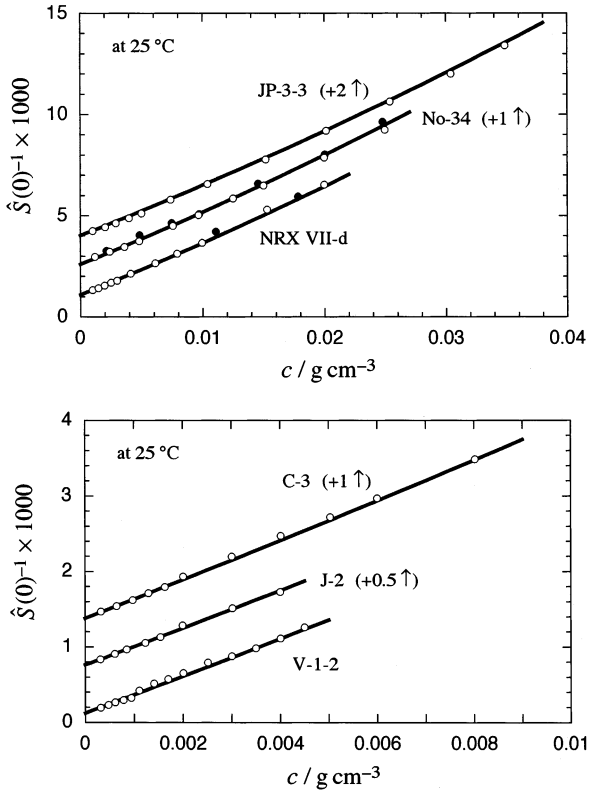

Figure 2. Polymer concentration dependence of $\hat{S}(0)^{-1}$ obtained for six PHIC samples. Key: unfilled circles, data obtained in the present study by light scattering; filled circles, $(M_0/RT)/(\partial\Pi/\partial c)$ data obtained previously by sedimentation equilibrium;[26] solid lines, theoretical values calculated by the scaled particle theory including the pertubation of a weak attractive interaction with $d = 1.10$ nm, $\delta = -(0.04 \pm 0.04)$ nm, and M_L (the molar mass per unit contour length) = 730 nm^{-1}.[26] Data points and theoretical lines for samples JP-3-3, No-34, C-3, and J-2 are shifted upward by the amount indicated in parentheses.

favorably compared with the scaled particle theory (SPT) including a perturbation term of the attractive interaction, using $M_L = 730$ nm^{-1},[23] d (the hard-core diameter) = 1.10 nm, and δ (the strength of the attractive interaction) = −0.01 nm.[27] As shown in Figure 2, light-scattering data for all PHIC samples examined obey the same theory with almost same molecular parameters, confirming the previous estimates of d and δ. The much smaller absolute value of δ than d indicates that the attractive interaction among PHIC molecules is very weak in *n*-hexane.

On the basis of the generalized Ornstein−Zernike integral equation theory (the GOZ theory), $\hat{S}(k)$ was formulated as[8]

$$\hat{S}(k)^{-1} = \frac{1}{N_0}\left[\frac{1}{P(\theta)} + \left(\frac{M}{RT}\frac{\partial\Pi}{\partial c} - 1\right)\right] \qquad (1)$$

where N_0, $P(\theta)$, and M are the degree of polymerization, the intramolecular interference factor, and the molecular weight of the polymer, respectively. As demonstrated by Murakami et al.,[20] $P(\theta)$ of PHIC in *n*-hexane at infinite dilution is favorably compared with the theoretical $P(\theta)$ for unperturbed wormlike chain model. Although $P(\theta)$ for flexible polymer chains in good solvents usually depends on the polymer concentration due to the screening effect of the excluded volume,[24] the chain stiffness of PHIC diminishes the excluded volume

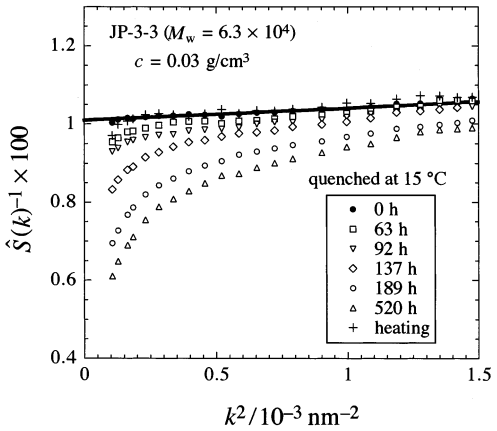

Figure 3. Plots of $\hat{S}(k)^{-1}$ vs k^2 for a *n*-hexane solution of sample JP-3-3 with $c = 0.03$ g/cm^3 quenched at 15 °C for various times. Key: solid line, theoretical values calculated by the GOZ theory with the same parameters as in Figure 1a; +, $\hat{S}(k)^{-1}$ (measured at 25 °C) of the solution quenched at 15 °C for 520 h and then heated at ca. 40 °C for ca. 10 h.

effect even in a good solvent, so that we can assume that $P(\theta)$ of PHIC in *n*-hexane is independent of c. Solid curves in Figure 1 indicate $\hat{S}(k)$ calculated by eq 1 with $P(\theta)$ obtained by the Yoshizaki−Yamakawa theory[28] for the unperturbed wormlike chain and with $\partial\Pi/\partial c$ calculated by the SPT as in Figure 2. The theoretical curves closely agree with the experimental data points for the two PHIC samples, though we have slightly changed q and M_L in the Yoshizaki−Yamakawa theory from the reference values in panel b. Similar agreements between theory and experiment of $\hat{S}(k)$ were obtained for other PHIC samples unless c is too high.

Anomalous Scattering. Figure 3 shows $\hat{S}(k)^{-1}$ (measured at 25 °C) of a *n*-hexane solution of sample JP-3-3 with $c = 0.03$ g/cm^3 before and after quenching at 15 °C for different times t_{quench}. Before quenching (filled circles), $\hat{S}(k)^{-1}$ obeys the GOZ theory as indicated by the solid line in the figure, and we cannot find any symptom of the anomaly in $\hat{S}(k)^{-1}$ of the solution. However, after quenching (unfilled symbols), $\hat{S}(k)^{-1}$ gradually deviates from the theoretical line with t_{quench}. The deviation is more remarkable at lower scattering angles θ, and the extrapolation of $\hat{S}(k)^{-1}$ to the zero θ becomes difficult. Although $\hat{S}(k)$ values for the quenched solution were identical at 15 and 25 °C, the solution recovered normal scattering after heating at ca. 40 °C for ca. 10 h, as shown by crosses in Figure 3. Thus, we conclude that the change occurring in the quenched PHIC solution is quasi-thermoreversible.

The t_{quench} dependence of $\hat{S}(k)$ at $k^2 = 1.06 \times 10^{-4}$ nm^{-2} ($\theta = 30°$) for the quenched solution in Figure 3 is shown by unfilled circles in Figure 4. The structure factor keeps increasing even after quenching for 500 h, indicating that the change occurring in the quenched PHIC solution is a quite slow process. After quenching for 520 h, the solution was heated at ca. 40 °C, and then quenched again at 15 °C. Filled circles in the same figure indicate $\hat{S}(k)$ at the same k^2 for the double quenched solution, confirming that the process is almost reproducible.

We have examined the dilution effect on $\hat{S}(k)$ of a *n*-hexane solution of sample JP-3-3 with $c = 0.030$ g/cm3 quenched at 15 °C for a long time. Figure 5 shows the change of $\hat{S}(k)^{-1}$ (at 25 °C) with dilution of the quenched solution to several concentrations at a room temperature (ca. 20 °C). The anomalous scattering behavior remains

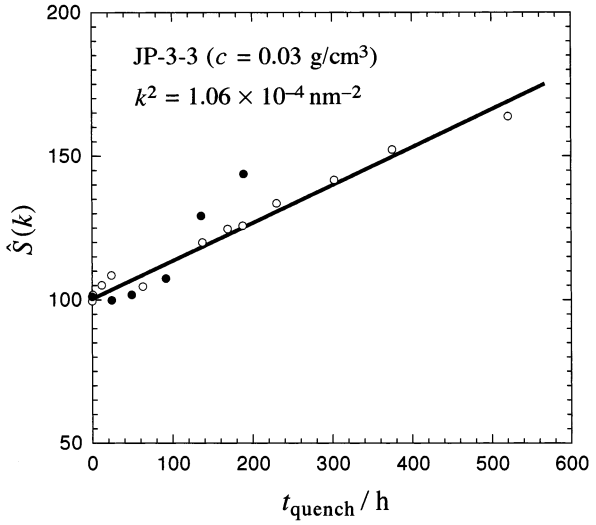

Figure 4. Time evolution of $\hat{S}(k)$ at $k^2 = 1.06 \times 10^{-4}$ nm^{-2} (θ = 30°) for the quenched solution shown in Figure 3.

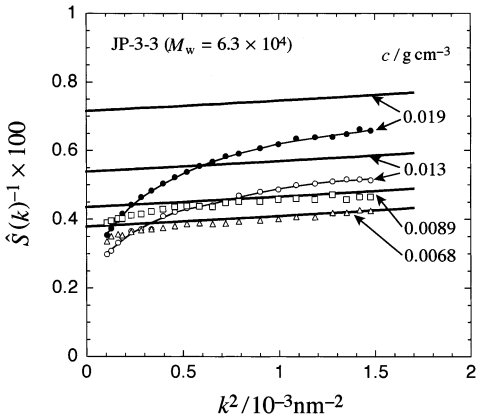

Figure 5. $\hat{S}(k)^{-1}$ for a quenched *n*-hexane solution of sample JP-3-3 after dilution to the concentrations indicated. Thick solid lines: theoretical values calculated by the GOZ theory with the same parameters as in Figure 1a.

in the solution diluted up to 0.013 g/cm^3, but further dilution remarkably weakens the k dependence of $\hat{S}(k)^{-1}$, and almost recovers the agreement between the experiment and GOZ theory (thick lines). The after-effect of quenching remains in $\hat{S}(k)^{-1}$ up to considerably low concentrations.

Figure 6 illustrates $\hat{S}(k)^{-1}$ for a *n*-hexane solution of higher molecular weight sample JP-3-1 with $c = 0.0105$ g/cm^3 quenched at 15 °C (unfilled symbols). In comparison with the same solution before quenching (filled circles), $\hat{S}(k)$ enhances at low k, and the angular dependence becomes stronger. For this solution, a small disagreement between experiment and the GOZ theory (the solid line) is observed at small k even before quenching. At $c < 0.03$ g/cm^3, the *n*-hexane solution of the lower-molecular-weight sample JP-3-3 exhibited no anomalous scattering by quenching at 15 °C. Therefore, we can say that the critical concentration of the occurrence of the anomaly is molecular-weight dependent. When the solution of sample JP-3-1 quenched at 15 °C for 15 h was diluted to $c = 0.0033$ g/cm^3, the enhanced low-angle scattering almost disappeared in $\hat{S}(k)$, as shown in Figure 6.

Figure 7 shows intensity autocorrelation functions $g^{(2)}(t)$ and their relaxation spectra $A(\tau)$ obtained by the CONTIN analysis of a solution of sample JP-3-3 with

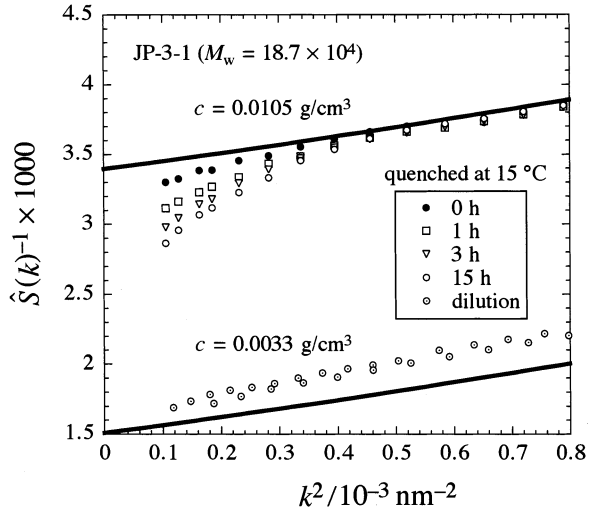

Figure 6. Plots of $\hat{S}(k)^{-1}$ vs k^2 for a *n*-hexane solution of sample JP-3-1 with $c = 0.01$ g/cm^3 quenched at 15 °C for different times. Solid line: theoretical values calculated by the GOZ theory with $q = 43$ nm, $M_L = 730$ nm^{-1}, $d = 1.10$ nm, and $\delta = -0.01$ nm.

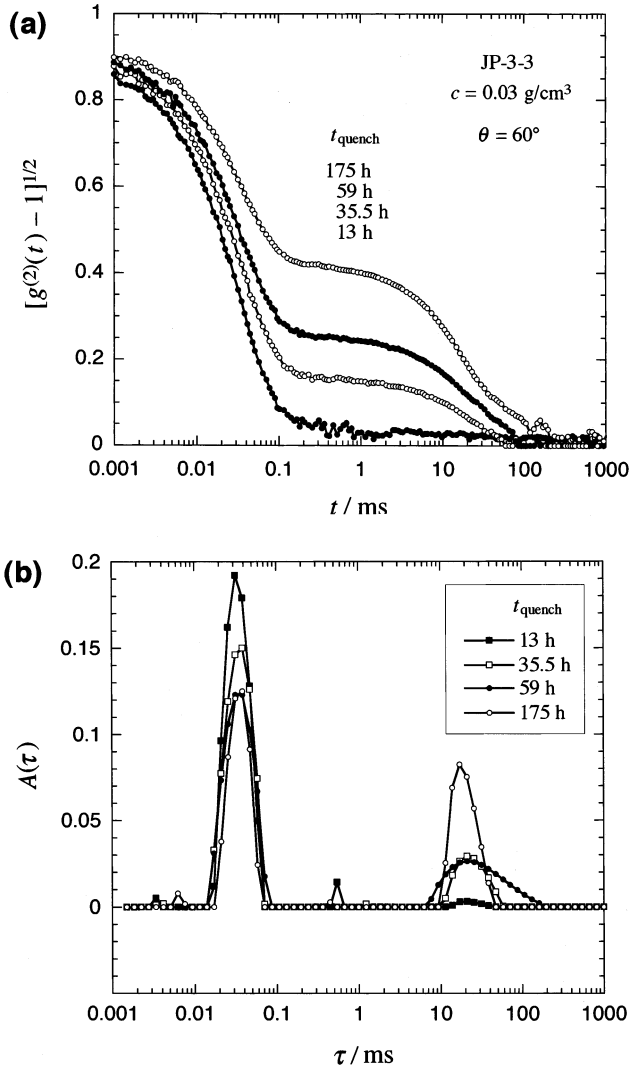

Figure 7. (a) Intensity autocorrelation functions $g^{(2)}(t)$ and (b) their relaxation spectra $A(\tau)$ of a solution of sample JP-3-3 ($c = 0.03$ g/cm^3) quenched for different times.

$c = 0.03$ g/cm^3 quenched at 15 °C for different times. At every t_{quench}, $A(\tau)$ is bimodal, and peak positions of both

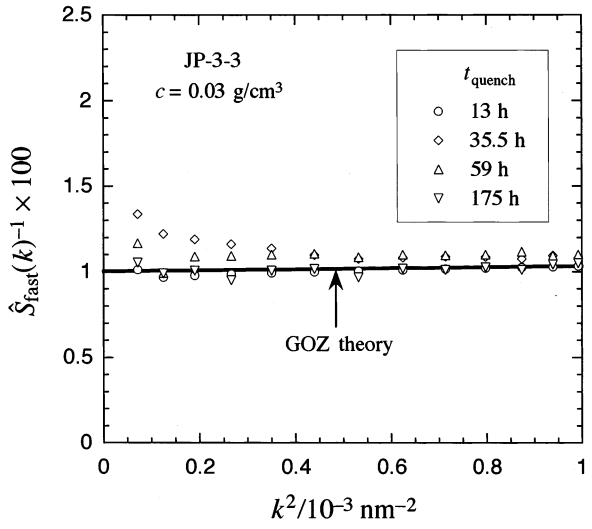

Figure 8. Fast relaxation mode component $\hat{S}_{fast}(k)$ of the static structure factor of the solution of sample JP-3-3 (c = 0.03 g/cm^3) quenched for different times. Thick line: theoretical values calculated by the GOZ theory with the same parameters as in Figure 1a.

fast and slow relaxation modes stay at almost constant τ independent of t_{quench}. On the other hand, the peak area of the slow relaxation mode, $\sum_{i\in slow}A(\tau_i)$, increases with t_{quench}, in accordance with the enhancement of the scattering intensity shown in Figure 3.[29] The slow relaxation mode in $A(\tau)$ indicates the existence of large scattering components in the quenched solution, which may cause the enhanced low-angle scattering. Furthermore, the almost constant position and gradually increasing area of the slow mode peak imply that sizes of the large scattering compoenents are essentially unaltered, but their amounts gradually increase in the quenched solution. Guenet et al.[30] reported bimodal $A(\tau)$ for quenched *n*-octane solutions of a PHIC sample, but their fast- and slow-mode peaks are broader than ours in Figure 7b. This difference may arise from different solvent condition and/or molecular weight heterogeneity in PHIC samples used.

Static light-scattering measurements were simultaneously made on the solution along with dynamic light-scattering measurements, and from the static and dynamic light-scattering results [i.e., $\hat{S}(k)$ and $A(\tau_i)$], we calculated fast relaxation mode components $\hat{S}_{fast}(k)$ of the static structure factor at different t_{quench} by

$$\hat{S}_{fast}(k) = \hat{S}(k) \sum_{i\in fast} A(\tau_i)/[\sum_{i\in fast} A(\tau_i) + \sum_{i\in slow} A(\tau_i)] \quad (2)$$

as functions of k. As shown in Figure 8, all $\hat{S}_{fast}(k)$ for different t_{quench}, indicated by different symbols, exhibit no enhanced low-angle scatttering and almost agree with the GOZ theory (the solid line), though slight upward deviations are seen in $\hat{S}_{fast}(k)$ for t_{quench} = 35.5 h at low-angles. From these results, we may conclude that the anomaly of $\hat{S}(k)$ in quenched *n*-hexane solutions of PHIC arises from some large scatterers formed in the solutions. Moreover, Figure 8 demonstrates that we can extract the normal scattering component from anomalous static light-scattering results with the assistance of dynamic light scattering.[31] It is noted that since the anomaly in $\hat{S}(k)$ disappears by dilution as shown in Figures 5 and 6, the hydrodynamic radius of the large scatterer formed in quenched solutions cannot be estimated by extrapolating the relaxation time of the slow mode to the zero polymer concentration.

Large scattering components formed in quenched *n*-hexane solutions may be aggregates or clusters of PHIC chains induced by some strong attractive force acting among the chains. Green et al.[16,17] found that a *n*-hexane solution of PHIC (molecular weight $\approx 3 \times 10^5$; $c = 5 \times 10^{-3}$ g/cm^3) forms a macroscopic gel at about -10 °C, which is a direct evidence for the strong attractive force among PHIC chains. However, this strong force seems to be inconsistent with the very small value of $|\delta|$ estimated in Figure 2. Moreover, PHIC has a more negative δ in dichrolomethane (DCM),[10,26] but DCM solutions of PHIC do not form thermoreversible gels but transform into a nematic state at high concentrations (>0.2 g/cm^3).[18,19] Thus, the aggregation or gelation of PHIC seems not to correlate to δ, and cannot be predicted by the thermodynamic theory which the GOZ theory is based on.

In part 3 of this series,[9] the attractive interaction potential $w(r)$ between two polymer chains was formulated using the theories of McLachlan[32,33] and Imura and Okano[34] on the dispersion interaction, and the attractive interaction parameter δ was calculated from this potential. The result of δ reads as

$$\delta \equiv \frac{4}{\pi}\int_d^\infty \left\langle \frac{w(r)}{k_B T} \left| \sin\gamma \right| \right\rangle dr = \delta_I + \delta_A \eta \quad (3)$$

where γ is the angle formed by unit tangent vectors **a** and **a′** of two interacting polymer chains at the closest contour points and η is the parameter depending on the orientation of **a** and **a′** defined by

$$\eta = \int\int d\mathbf{a}\, d\mathbf{a}'\, P_2(\mathbf{a}\cdot\mathbf{a}')\bar{f}(\mathbf{a})\bar{f}(\mathbf{a}') \quad (4)$$

with the orientational distribution function $\bar{f}(\mathbf{a})$ of **a** and the second Legendre polynomial $P_2(x)$. The coefficients δ_I and δ_A in eq 2 represent strengths of the isotropic and anisotropic components of δ, respectively. When two interacting polymer chains are oriented randomly, η is equal to zero, and the anisotropic component does not contribute to δ. The value of δ estimated in Figure 2 in molecularly dispersed isotropic solutions of PHIC should be identified with δ_I in eq 3. On the other hand, if two chains align parallel each other in aggregates, the contribution of the anisotropic component to δ in eq 3 becomes important. Therefore, eq 3 indicates that the attractive interaction in aggregates is not necessarily identical with that in molecularly dispersed isotropic solutions.

To examine the chain alignment in PHIC aggregates, we made depolarized light-scattering measurements for a PHIC solution but did not detect any difference in the anisotropic scattering before and after quenching of the solution. However, this result does not necessarily indicate no chain alignment in PHIC aggregates, because the anisotropic scattering is in general not so sensitive to a tiny amount of aggregates, unlike the isotropic scattering.[35,36]

No correlation between the aggregation and the solvent quality (or the Flory−Huggins interaction parameter) was also reported for polystyrene solutions.[11−14] The origin of the strong attractive force between polystyrene chains in the gel or aggregate is still a matter in dispute. Guenet et al.[11,14] insisted that the strong attraction may result from the formation of solvated

crystals of polystyrene. The aggregation of PHIC is also very sensitive to the solvent. For example, gelation takes place in *n*-octane solutions of PHIC at higher temperatures than in *n*-hexane solutions of PHIC.[16] Therefore, the solvent may play an important role, and the interaction between PHIC and *n*-hexane must be studied to elucidate the role of the solvent in the aggregation of PHIC in future.

References and Notes

(1) Ohta, T.; Nakanishi, A. *J. Phys. A: Math. Gen.* **1983**, *16*, 4155.
(2) Nakanishi, A.; Ohta, T. *J. Phys. A: Math. Gen.* **1985**, *18*, 127.
(3) des Cloizeaux, J.; Jannink, G. *Polymers in Solution. Their Modelling and Structure*; Clarendon Press: Oxford, England, 1990.
(4) Schweizer, K. S.; Curro, J. G. *Phys. Rev. Lett.* **1987**, *58*, 246.
(5) Curro, J. G.; Schweizer, K. S. *Macromolecules* **1987**, *20*, 1928.
(6) Curro, J. G.; Schweizer, K. S. *J. Chem. Phys.* **1987**, *87*, 1842.
(7) Honnell, K. G.; Curro, J. G.; Schweizer, K. S. *Macromolecules* **1990**, *23*, 3496.
(8) Sato, T.; Jinbo, Y.; Teramoto, A. *Polym. J.* **1995**, *27*, 384.
(9) Sato, T.; Jinbo, Y.; Teramoto, A. *Polym. J.* **1999**, *31*, 285.
(10) Jinbo, Y.; Sato, T.; Teramoto, A. *Macromolecules* **1994**, *27*, 6080.
(11) Guenet, J.-M.; Willmott, N. F. F.; Ellsmore, P. A. *Polym. Commun.* **1983**, *24*, 230.
(12) Koberstein, J. T.; Picot, C.; Benoit, H. *Polymer* **1985**, *26*, 673.
(13) Gan, J. Y.; François, J.; Guenet, J.-M. *Macromolecules* **1986**, *19*, 173.
(14) Guenet, J.-M. *Thermoreversible Gelation of Polymers and Biopolymers*; Academic Press: London, 1992.
(15) Heckmeier, M.; Strobl, G. *Macromolecules* **1997**, *30*, 4454.
(16) Green, M. M.; Khatri, C. A.; Reidy, M. P.; Levon, K. *Macromolecules* **1993**, *26*, 4723.
(17) Green, M. M.; Peterson, N. C.; Sato, T.; Teramoto, A.; Cook, R.; Lifson, S. *Science* **1995**, *268*, 1860.
(18) Conio, G.; Bianchi, E.; Ciferri, A.; Krigbaum, W. R. *Macromolecules* **1984**, *17*, 856.
(19) Itou, T.; Teramoto, A. *Macromolecules* **1988**, *21*, 2225.
(20) Murakami, H.; Norisuye, T.; Fujita, H. *Macromolecules* **1980**, *13*, 345.
(21) Actually molecular weights and radii of gyration were determined from plots of $\partial^{-1/2}$ vs k^2, because of wider linear region of the root plots.
(22) Benoit, H.; Doty, P. M. *J. Phys. Chem.* **1953**, *57*, 958.
(23) Norisuye, T.; Tsuboi, A.; Teramoto, A. *Polym. J.* **1996**, *28*, 357.
(24) de Gennes, P.-G. *Scaling Concepts in Polymer Physics*; Cornell University Press: Ithaca, NY, 1979.
(25) Fujita, H. *Polymer Solutions*; Elsevier: Amsterdam, 1990; Vol. 9.
(26) Sato, T.; Jinbo, Y.; Teramoto, A. *Macromolecules* **1997**, *30*, 590.
(27) In ref 26, the sedimentation equilibrium data were analyzed by incorporating the effects of polymer chain ends and polydispersity. The former effect was negligible at $M_w \gtrsim 1 \times 10^4$, while the latter effect was not important for fractionated PHIC samples used previously. In Figure 2, we have neglected these two effects.
(28) Yoshizaki, T.; Yamakawa, H. *Macromolecules* **1980**, *13*, 1518.
(29) Although there are some very small peaks other than the two main ones in $A(\tau)$ shown in Figure 6b, we did not regard them as realistic relaxation components but as artificial noises through the CONTIN analysis.
(30) Guenet, J.-M.; Jeon, H. S.; Khatri, C.; Jha, S. K.; Balsara, N. P.; Green, M. M.; Brulet, A.; Thierry, A. *Macromolecules* **1997**, *30*, 4590.
(31) Strictly speaking, the fast and slow mode peaks cannot always simply assign to small and large scattering components, respectively, for solutions of finite concentrations.[37−40] The theoretical justification of the results of Figure 7 will be given in a separated paper.[41.]
(32) McLachlan, A. D. *Proc. R. Soc. London* **1963**, *A271*, 387.
(33) McLachlan, A. D. *Proc. R. Soc. London* **1963**, *A274*, 80.
(34) Imura, H.; Okano, K. *J. Chem. Phys.* **1973**, *58*, 2763.
(35) Nagai, K. *Polym. J.* **1972**, *3*, 67.
(36) The anisotropic scattering intensity depends on the shape of aggregates. The depolarized light-scattering experiment may not detect a tiny amount of aggregates, unless the aggregates are very straight fiberlike, where x^{-1} in eq 83 of ref 35 becomes very large.
(37) Benmouna, M.; Benoit, H.; Duval, M.; Akcasu, Z. *Macromolecules* **1987**, *20*, 1107.
(38) Foley, G.; Cohen, C. *Macromolecules* **1987**, *20*, 1891.
(39) Sun, Z.; Wang, C. H. *Macromolecules* **1996**, *29*, 2011.
(40) Sun, Z.; Wang, C. H. *Macromolecules* **1997**, *30*, 4939.
(41) Kanao, M.; Matsuda, Y.; Sato, T. *Macromolecules*, submitted for publication.

MA020704O